Measurement-based Modeling of Packet Inter-Reception Time in Presence of Radio Channel Congestion

Federico Librino, **M. Elena Renda**, **Paolo Santi**
E–mail: {name.surname}@iit.cnr.it

***Abstract*—In this paper, we study the performance of the beaconing mechanism underlying active safety vehicular applications in presence of different levels of channel congestion. The importance of this study lies in the fact that channel congestion is considered a major factor influencing communication performance in vehicular networks, and that ours is the first investigation of the effects of congestion based on extensive, real-world measurements.**

We present a set of measurement-based models of the packet inter-reception time, and we show how these models can be used to estimate the application-level benefits, expressed in terms of increased reliability, of congestion control and of multi-hop propagation of situational information.

I. Introduction

Active safety applications are a class of vehicular applications aimed at improving a driver's situation awareness, and road safety conditions in general. Applications belonging to this class build on top of a low-level beaconing mechanism, according to which each vehicle periodically broadcasts its status information (position, kinematic data, etc.) to surrounding vehicles. The effectiveness of the beaconing mechanism[1], which can be informally understood as the extent to which a vehicle is *promptly* informed of the status of *all* surrounding vehicles, is the pre-requisite for any active safety application to meet its often strict design requirements. The importance of beaconing is well understood within the vehicular networking community, which has devoted substantial efforts to characterizing its performance initially by means of analysis/simulation [3], [8], [16] and, more recently, based on real-world measurements [1], [12].

Early studies on beaconing performance [8], [16] have revealed that the beaconing mechanism itself, if not adequately designed, can cause channel congestion in presence of medium to dense vehicular traffic conditions. In turn, channel congestion can severely degrade beaconing effectiveness, potentially impairing the strict communication requirements imposed by active safety applications running on top of beaconing. For this reason, congestion control protocols have been proposed in the literature, with the goal of tuning communication parameters (such as transmission power, beaconing rate, etc.) in order to confine channel congestion below a certain threshold perceived as corresponding to "acceptable" channel conditions. For instance, ETSI indicates a Channel Busy Time (CBT) $\leq 25\%$ as an "acceptable" congestion level for active safety applications [4]. For an overview of the congestion control problem and relative solutions, the interested reader is referred to [13].

Despite the body of literature devoted to congestion control in vehicular networks, very little is known to date on the effects of congestion level on beaconing performance *in a real-world scenario*. In fact, all studies on congestion control we are aware of are based only on analysis, simulation, or on their combination. On the other hand, it is well-known that analysis/simulation alone cannot fully capture the complexity of a real-world vehicular environment, and measurements taken during real-world vehicular network deployments can lead to a better understanding of vehicular link performance. For instance, measurement-based studies have highlighted the negligible effect of spatio/temporal correlation on PDR link performance [1], while, on the contrary, LOS/NLOS conditions have been shown to have a notable effect on the link [11], [12].

In this paper, we make a step towards filling this gap and present, to our best knowledge, the first measurement-based study of beaconing performance in presence of different levels of channel congestion. The goal of the study is gaining an understanding and deriving a model of how the packet inter-reception time (PIR) is impacted by radio channel congestion, including possible use of multi-hop forwarding of situational information to improve beaconing performance. Focusing the study on the packet inter-reception time is justified by the observation made in [3], [12] that PIR time is the most important beaconing metric, as well as by the fact that important classes of active safety applications, such as collision warning, mandate requirements in terms of the maximum tolerable PIR time [14].

The measurement-based PIR time model is then used to derive accurate bounds to the frequency of experiencing "situational-awareness" blackouts by means of a Markov-Chain based approach. Finally, we show how the derived bounds on blackout frequency can be used to estimate the

[1]A message carrying the information concerning position and status of a vehicle is called Cooperative Awareness Message (CAM) according to the European ETSI-ITS standard [4], or Basic Safety Messages according to the American DSRC standards [2], respectively.

reliability of a forward collision warning application in presence of different levels of channel congestion.

II. Related work

The problems of estimating beaconing performance in presence of channel congestion [8], [16], and of designing congestion control protocols [7], [9], [13], [15], [17], have been extensively studied in the literature. To our best knowledge, however, all existing studies are based on analysis, on simulation, or on their combination.

Measurement-based investigation of beaconing performance has been addressed in a few recent papers. In [6], the authors consider an intersection collision warning application, and evaluate PDR and RSSI as a function of the distance of the two vehicles from the intersection. In a similar study [11], Mangel et al. evaluates how NLOS conditions impact PDR and RSSI as vehicles approach an intersection. The effects of visibility conditions on channel quality are studied also in [5], where the authors focus on vehicle-to-infrastructure communications. The focus in [14] is in characterizing the reliability of different active safety applications based on real-world measurements.

In [1], the authors present an extensive analysis of PDR in different scenarios for what concerns propagation environment, data rate, etc. The authors also analyze temporal, spatial, and symmetric correlation of PDR values, and conclude that, while temporal and spatial correlation are weak, symmetric correlation is instead quite strong.

In a previous work [12], some of the authors of this paper have characterized beaconing performance not only in terms of PDR, but also in terms of the most relevant PIR metric. In [12], it is shown that PDR and PIR are loosely correlated metrics, thus indicating that PDR cannot be used as a representative metric of situation-awareness.

To our best knowledge, all measurements reported in the literature are performed with few vehicles communicating in a *congested-free channel*. Thus, characterizing real-world beaconing performance in presence of a congested channel, and its impact on active safety applications, is still an open problem.

III. Measurement Methodology

The goal of the measurements is to derive a PIR time model in presence of different levels of radio channel congestion. Channel congestion is quantified in terms of Channel Busy Time (CBT), which is defined as the average fraction of time that the channel is sensed as busy. In order to generate values of the CBT around 25%, which is the maximum acceptable limit for CBT according to ETSI recommendations, a number of transmitting vehicles in the order of several tens would be needed [15]. Using such a large number of vehicles in a real-world experiments is highly challenging, due to cost as well as logistic issues. For this reason, we have decided to *emulate* the transmission of beaconing packets by a large number of vehicles by having two vehicles (*interferer vehicles*) transmitting CBR traffic with increasing rates.

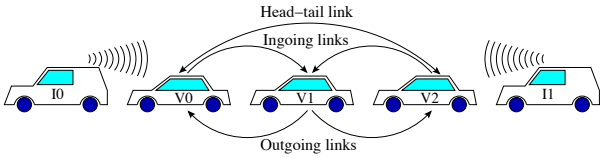

Fig. 1. Reference vehicles configuration for experiments with background traffic.

More specifically, the vehicle configuration used in the experiments is reported in Figure 1. Three experiments were performed with a five vehicle configuration and constant R background traffic, with CBR adjusted to have a value of R of $500\,kbps$, $650\,kbps$ and $800\,kbps$ during the three experiments, corresponding to channel busy time values of 18%, 24% and 29%, respectively. A fourth experiment was performed using only beaconing vehicles (vehicles V_0, V_1, V_2 in Figure 1) and no background traffic, to estimate the baseline beaconing performance in absence of channel congestion. While we could have used data from previous measurement campaigns [12] to estimate baseline beaconing performance, we decided to undertake a more rigorous approach using exactly the same vehicle configuration and hardware devices used during the five vehicle experiments, so to rule out possible effects of vehicle heights and inhomogeneous hardware performance.

Notice that interferer vehicles I_0 and I_1 were placed at the head and tail of the platoon. Notice also that I_0 and I_1, with an approximate height of $1.75\,m$ and $2.07\,m$, were significantly taller than the beaconing vehicles V_0, V_1 and V_2, whose heights were $1.45\,m$, $1.46\,m$ and $1.54\,m$, respectively. Using relatively taller vehicles in head and tail position was a design choice made to generate as a uniform traffic floor as possible for the three vehicles under test V_0, V_1 and V_2. As mentioned above, vehicles I_0 and I_1 were intended to mimic a background traffic which is likely to be present in a wider vehicular network, where also surrounding vehicles actively transmit and receive data packets. While admittedly not able to replicate the complex dynamic of a large scale CSMA/CA network with tens of vehicles, using emulated background traffic is a reasonable compromise between accuracy and cost of the vehicular network deployment.

1) **Hardware configuration:** Experiments were performed with a hardware setup similar to that described in [12], which has been extended to five vehicles instead of two. For vehicular communications, in each vehicle we used a IEEE 802.11p compliant NEC LinkBird-MX unit, an omnidirectional WiMo antenna ($108\,mm$ long, $5\,dBi$ gain), a laptop, and a GPS receiver. Channel 180 at $5.9\,Ghz$ (the control channel, recommended for safety applications) was selected for radio communication among vehicles. The transmission power was fixed to $20\,dBm$, with a $3\,Mbps$

PHY layer data rate and a $10\,Mhz$ channel bandwidth.

The antennas were installed at the centre of the roofs for the three beaconing vehicles V_0, V_1, and V_2, as recommended in [11]. For the interferer vehicles I_0, I_1, the antennas were shifted in the direction of the three beaconing vehicles, in order to increase the impact of congestion on the beaconing process.

2) **Multihop beaconing application:** In the experiments, we have implemented a *multi-hop* beaconing application through a Java application running on each vehicle. The application piggy-backs in the beacon sent by vehicle V situational information about other vehicles from which V has received beacons. As the results of our study show, piggy-backing situational information is an effective means of relieving the negative effect of radio channel congestion on beaconing performance.

The multi-hop propagation of data inherently requires two main elements. On the one hand, the usage of an efficient data structure is necessary to keep the information about surrounding vehicles updated; on the other hand, an effective way of including this information (or a portion of it) in the beacons has to be designed, without violating the constraint on the beacon size, which is fixed to $100\,B$. In fact, the designed multi-hop beaconing application satisfies the property that piggy-backing of situational information should not negatively impact on channel congestion by increasing beacon size.

If V is the considered vehicle, we define as $\mathcal{R}(V)$ the subset of vehicles whose beacon packets carry relevant information for V. The elements in $\mathcal{R}(V)$, as well as its cardinality, are not fixed, but change over time. For this reason, we used the JAVA `HashMap` dynamic data structure, storing and managing `<key,value>` pairs. We use the vehicle ID as `key`, being uniquely associated to a given vehicle, and the corresponding *situational information* as the `value`, this consisting of the ID of the last received packet ($4\,B$), *latitude* ($4\,B$), *longitude* ($4\,B$), *speed* ($4\,B$), *heading* ($4\,B$) and *GPStime* ($8\,B$).

Even if the number of entries in a `HashMap` may vary, in our experiments we fix it to 3, since we know in advance that only three out of the five vehicles are sending beacons. The resulting beacon contains: *(i)* the sender vehicle ID ($1\,B$); *(ii)* the number of vehicles (up to three in our experiments) whose *situational information fields (SIF)* are included in the beacon ($1\,B$); and *(iii)* the SIFs of each beaconing vehicle, including the sender. The total beacon payload is $89\,B$, which is finally padded to $100\,B$, as shown in Figure 2.

Notice that including situational information about n surrounding vehicles in a beacon without increasing its size is not possible as long as $n > 3$. However, in [10] it is shown that network coding techniques can be effectively used to improve beaconing performance while not exceeding the allowed beacon size also when $n > 3$.

The beaconing application running on each vehicle triggers the transmission of a new beacon every $100\,ms$, and records beacons received from other vehicles, as well as those transmitted from the vehicle itself.

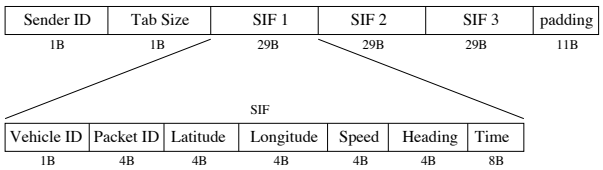

Fig. 2. Beacon format.

3) **Experiment setup:** We performed four different experiments, conducted during four Pisa-Florence-Lucca trips. Each trip was about $160\,km$ long, and consisted of two parts: the former was on a freeway from Pisa to Florence, with speed limit of $90\,km/h$ and two lanes per direction, while the latter was on a highway from Florence to Lucca, with speed limit of $130\,km/h$ and two/three lanes per direction.

Since beacons are broadcast, we can identify 6 different beaconing links between beaconing vehicles – see Figure 1: the *outgoing links* from V_1 towards V_0 and towards V_2; the *ingoing links* from V_0 and V_2 towards V_1; and the (bidirectional) link between V_0 and V_2, the *head-tail link*, possible even if the presence of V_1 often blocks the LOS between V_0 and V_2.

Each link (V_i, V_j) described above, with $i, j \in \{0, 1, 2\}$, is a physical link, and its performance can be measured by analyzing the beaconing packets transmitted by V_i and received by V_j. However, the presence of a third beaconing node V_k makes it possible to define also a corresponding multi-hop link $(V_i, V_j)_{MH}$, which takes into account also the packets sent by V_i which are not directly received by V_j, but instead delivered via relaying through the path $V_i - V_k - V_j$. Although multi-hop is more relevant for the *head-tail* link, the augmented diversity offered by relaying can be beneficial also for the other links, as will be shown later.

In [12], it has been observed that the PIR time is not correlated to the distance between vehicles, as long as the vehicles remain within each other transmission range. For this reason, in the experiments PIR time measurements referring to, say, link (V_i, V_j) are aggregated across all inter-vehicle distances.

IV. Impact of wireless channel congestion

We first investigate the effect of different wireless channel congestion levels on PIR time.

In Figure 3, the complementary cumulative distribution function (ccdf) of the PIR time over the head-tail links is shown. A first observation concerns the shape of the distribution, which is strongly influenced by radio channel congestion: while *the PIR time ccdf behaves like a power law without congestion* (confirming what found in [12]), *the distribution behaves like a power law with exponential cutoff in presence of congestion*. While we defer a more accurate modeling of the PIR time distribution in presence

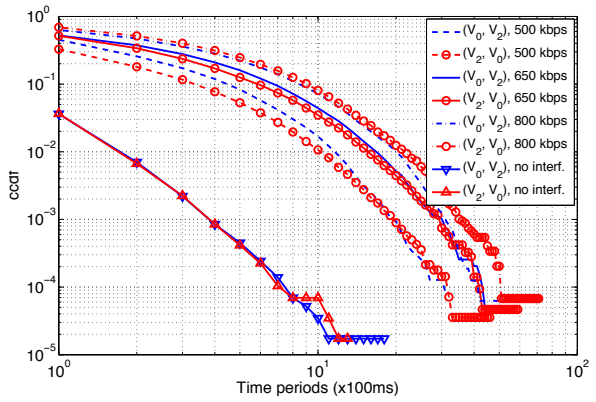

Fig. 3. PIR time ccdf of the head-tail links for different wireless channel congestion levels.

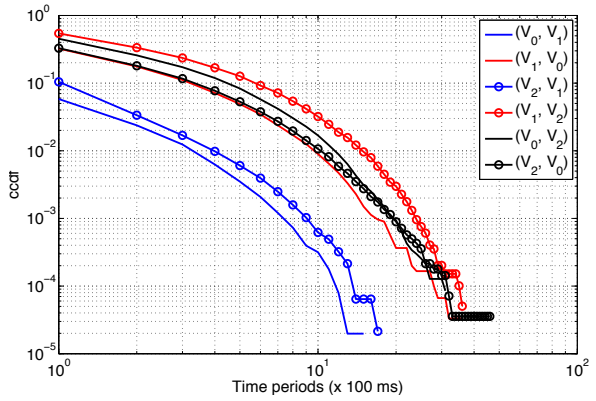

Fig. 4. PIR time ccdf of the six vehicular links, when the congestion level is fixed to $R = 500\,kbps$.

of congestion to Section VI, we would like to emphasize here that, while the exponential cutoff of the distribution tail caused by congestion might hint to a thinner tail of the PIR time ccdfs with congestion as compared to the congestion-free distribution, this is not actually the case. As reported in Figure 3, channel congestion severely impacts the *head* of the PIR distribution, implying that the tail of the PIR distribution with congestion, despite its exponential trend, is still fatter than the tail of the congestion-free distribution.

From Figure 3, we also observe that the PIR time distribution *does not depend on the link direction*. A small difference between the link (V_0, V_2) and the link (V_2, V_0) is observed only for the congestion level $R = 500\,kbps$, with a slightly worse performance for the former.

To gain a better understanding on the effect of link directionality at intermediate congestion levels, we analyze the PIR time ccdf of the six links when congestion level is $R = 500\,kbps$ – see Figure 4. We first observe that *incoming links ((V_0, V_1) and (V_2, V_1)) consistently experience a better performance than the other links*. This is due to the fact that these links are relatively short, and that they are unlikely to experience the hidden terminal problem. In fact, transmitter vehicles (either V_0 of V_2) are relatively close to the source of background traffic, implying that, when gaining access to the channel, the respective interferer vehicle (I_0 for V_0 and I_1 for V_2) is likely to sense the ongoing beaconing transmission, refraining from transmitting background traffic. Conversely, hidden terminal is likely to be the cause of the bad performance experienced by outgoing links ((V_1, V_0) and (V_1, V_2)). In this case, transmitter vehicle V_1 is relatively far from the two interferers; hence, its beacon transmission is likely not to be sensed by I_0 and/or I_1. Thus, interferers might not refrain from transmitting background traffic during V_1's transmission, causing interference at the receiver vehicles V_0 and/or V_2. It is interesting to observe that hidden terminal effect slightly outweighs also the effect of NLOS, since performance of link (V_1, V_2) is slightly worse than that of the longer, and likely NLOS, link (V_0, V_2).

V. Impact of multihop beaconing

In a real vehicular network, especially in presence of medium to heavy traffic, several vehicles are likely to communicate within the same area. Having a large number of communicating vehicles might cause channel congestion problems which, as shown in the previous section, can severely impact beaconing performance. Spatial diversity can be exploited as a way of counteract this effect. When multi-hop beaconing is employed, each node includes in its beaconing packets information about surrounding vehicles, thus actually relaying the beacons sent from other nodes. As a result, the same information can be delivered to the same vehicle through different paths, obtaining a substantial performance improvement if the direct link is weak.

As described in Section III, our beaconing application includes in the beacon the information of all the three beaconing vehicles. In case multi-hop performance is evaluated, we derived the PIR on link $(V_i, V_j)_{MH}$ considering all the entries of the output file generated by the beaconing application running on V_j. By doing this, we took into account all the updates regarding the situational information of V_i in the `HashMap` on V_j, no matter whether the beaconing packet which triggered the update was generated from V_i. On the contrary, when the performance of simple beaconing is evaluated[2], we filtered the output file written by V_j to contain only the lines corresponding to updates in the `HashMap` due to beacons received from V_i.

Figure 5 depicts the ccdf of the PIR on the link (V_0, V_2), with and without multi-hop beaconing. The same performance has been observed for the (V_2, V_0) link. As expected, multi-hop beaconing offers a relevant improvement in all the considered scenarios. In particular, we observe that when congestion level is low ($R = 500\,kbps$), or even absent, the entire ccdf curve is shifted downwards. In this situation, the impact of congestion on beaconing performance is not overwhelming, and the effect of the more frequent NLOS conditions on (V_0, V_2) is still relevant. When multi-hop is

[2]The data reported in Section IV refers to simple beaconing.

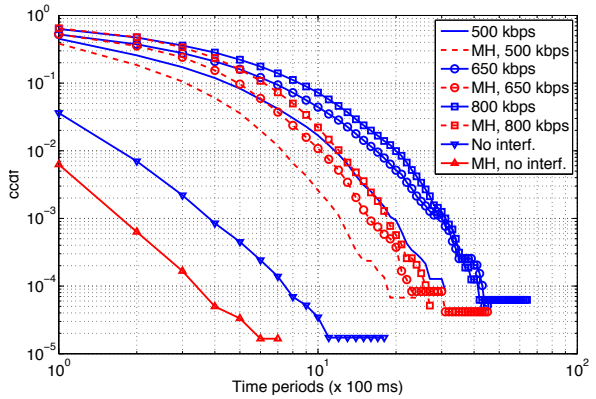

Fig. 5. PIR time ccdf on the (V_0, V_2) link, with and without multi-hop beaconing, for different levels of congestion.

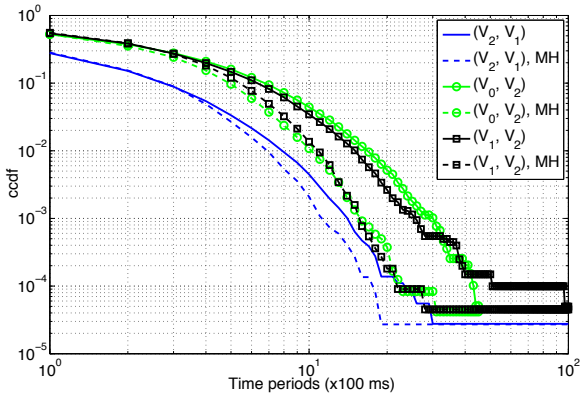

Fig. 6. PIR time ccdf of the links from and towards V_2 when $R = 650\,kbps$, with and without multi-hop beaconing.

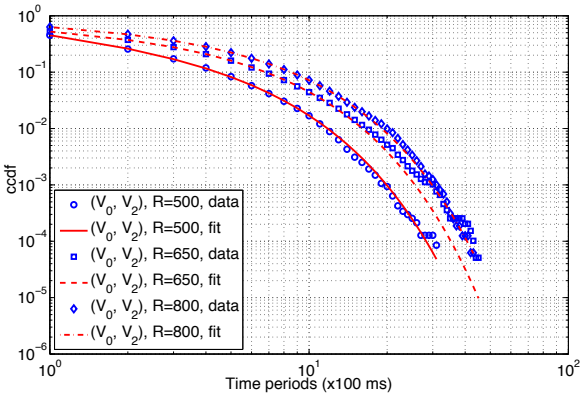

Fig. 7. PIR time ccdf of link (V_0, V_2) for different congestion levels: measured data and fitting curves.

used, shorter links are involved, where in addition LOS is often available, thus highly reducing the average PIR, especially for the scenario with no interferers.

When congestion level is higher ($R = 650\,kbps$ and $R = 800\,kbps$), its effect on beaconing performance becomes predominant. In this case, the multi-hop curves show a considerable improvement only in the tails. In fact, even if we can assume that link (V_0, V_1) is more reliable, due to vehicle configuration, the two links (V_0, V_2) and (V_1, V_2) are hampered by the same interferer node (I_1). Therefore, each of them is likely to experience relatively long PIRs. However, assuming that the fading coefficients of the two channels are almost uncorrelated, the average time necessary to decode a packet over either one of the two links is statistically lower. This explains why the spatial diversity benefit then becomes more evident in the ccdf tails. In absolute terms, *multihop beaconing reduces the probability of experiencing a black-out event ($PIR > 10$) of approximately one order of magnitude*, with a relatively smaller reduction in black-out probability for relatively higher congestion level.

In scenarios with a high interference level, as observed, relaying can be beneficial. It is worth noting that this beneficial effect may not be limited to the *head-tail* links. In Figure 6, the ccdf curves of the PIR over the links from and towards V_2 are reported, when $R = 650\,kbps$.

We have already commented on the benefits on multihop beaconing on link (V_0, V_2). However, measurements show that an improvement of beaconing performance with multihop is clearly visible also for links (V_1, V_2) and (V_2, V_1). Interestingly, the beneficial effect of multihop beaconing is more visible on the problematic (V_1, V_2), showing that *spatial diversity can be effectively used to lessen the impact of the hidden terminal problem*.

VI. Modeling Congested Links

As observed in Section IV, the shape of the PIR time distribution is clearly influenced by congestion: while, as observed in [12], it behaves like a power law in absence of congestion, it instead follows a power law with exponential cutoff in presence of congestion. Here we assess the latter statement, showing how well the measurement data can be fitted by the following power law with exponential cutoff:

$$\mathbb{P}[PIR > k] = ak^{-b}e^{-ck} \tag{1}$$

where a, b and c are parameters to be determined. More precisely, a and b jointly influences the ccdf behavior for low PIR values, which is close to that of a power law, while c determines the shape of the distribution tail. On the grounds of the measured data, we performed an iterative procedure based on Gauss-Newton algorithm to derive the three parameters of the distributions which best approximate the curves of interest.

As an example, we report in Figures 7 and 8 the ccdf of the PIR in some of the analyzed cases. In Figure 7 we plot the ccdf of the PIR on link (V_0, V_2), for different levels of congestion. The curves obtained through proper selections of the parameters a, b and c are always quite accurate, which confirms the good approximation offered by a power law with exponential decay. The same can be observed for the PIR ccdf of ingoing and outgoing links, with and without multi-hop beaconing, as illustrated in Figure 8.

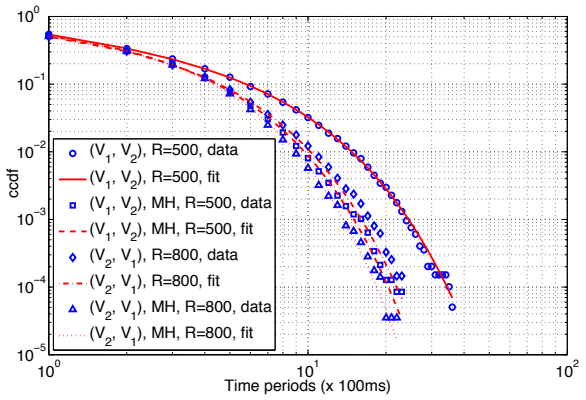

Fig. 8. PIR time ccdf of link (V_1, V_2) and (V_2, V_1) for different congestion levels, with and without multi-hop beaconing: measured data and fitting curves.

After deriving the optimal parameters for all the curves, we can make the following observations:

- when increasing the congestion level, the value of a also quickly increases, while b becomes lower and c is unaffected or does not show a clear trend. This is consistent with the fact that congestion mainly impacts on low PIR values, being large PIR values also due to link length or NLOS conditions;
- when enabling multi-hop beaconing, both a and b show very small variations (a slightly increases, b slightly decreases), while c become much higher (often more than doubled). This confirms that multi-hop is particularly effective in reducing the distribution tail, where spatial diversity can offer the highest benefits, as explained in Section V;
- the values of a are relatively larger for outgoing links than for the ingoing links, while the opposite holds for the values of b, as expected, since the outgoing links are relatively more impaired by congestion;
- when congestion is not present, the ccdf curves are approximated by a power law, which can be obtained from the general expression in (1) by setting $c = 0$. This is consistent with the results assessed in [12].

VII. Modeling Black-Out Events

In this section, we use the PIR time model defined in the previous section to derive a Markov-Chain based model of black-out events. Black-out events are defined as occurrence of a PIR time exceeding a threshold. Their importance lies in the fact that some classes of active safety applications, such as the forward collision warning application considered in the next section, specify requirements in terms of maximum tolerable PIR time. Hence, blackout events can be used to characterize the reliability of such class of applications. Although the model presented in the following can be used in combination with any duration of the blackout event, for definiteness and in accordance with [12] we define a blackout event as a PIR time $> 1sec$, corresponding to loosing at least $\ell = 10$ consecutive beacons.

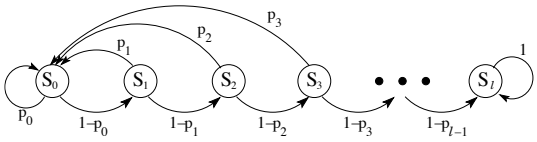

Fig. 9. Graphical representation of the MC modeling process $\mathcal{H}$.

In the following, we analyze the black-out statistics collected during the experiments, and compare these with predictions obtained from different models. The first considered black-out model is the one proposed in [12], according to which the average inter-black out time T_{bo}, defined as the average interval between two successive black-outs, can be estimated as follows:

$$T_{bo} = \mathbb{E}[PIR] \cdot \frac{1}{p_{bo}} \ , \tag{2}$$

where $p_{bo} = \mathbb{P}[PIR > \ell]$ is the black-out probability[3] and $\mathbb{E}[PIR]$ is the expected PIR time, both derived from the measured PIR time distribution. In fact, a new PIR value is expected to be observed every $\mathbb{E}[PIR]$ seconds and, assuming independence of black-out events, we can model them as Bernoulli trials.

Indeed, equation (2) is inaccurate, due to the fact that, as observed in [12], black-out events *are not* independent. In fact, black-outs are typically caused by bad channel conditions, which usually show strong temporal correlation. Hence, the expression in (2) can be considered an upper bound to the actual inter-blackout time, which is tighter in scenarios with low channel congestion. In fact, in such scenarios black-outs occur with relatively low probability, T_{bo} is larger, and the temporal correlation between two subsequent black-outs is lower. On the contrary, when interference is high, channel conditions are worse, black-outs are much more frequent, and also their time correlation increases. As a result, the expression in (2) becomes too optimistic in presence of congestion. The results presented in the remainder of this section confirm this intuition.

A different approach to model black-out events, which partially takes into account the channel time-correlation, is based on Markov Chain (MC). We can define a Markov process $\mathcal{H}$ to model beaconing packet reception as follows. Consider a process with states S_i, $0 \leq i \leq \ell$. A state change occurs every time a new beacon is sent from the transmitter to the receiver. The process is in state S_i if the last i beacons have been lost. Therefore, the corresponding MC is represented in Figure 9.

Note that state S_ℓ is an absorbing state, and correponds to a black-out event. As a result, the average time between two

[3]In the following, we assume that the PIR can take only values in $\mathbb{Z}^+(T_B)$, that is, multiples of the inter-beaconing period $T_B = 100\,ms$. Therefore, we omit the term T_B and consider $\mathbb{P}[PIR > \ell]$ as the probability that PIR is larger than $\ell \cdot T_B$.

subsequent black-outs can be approximated by the expected absorbing time of the MC, starting from state S_0.

In order to do this, the transition probabilities p_i, with $0 \leq i \leq \ell-1$ are to be known. These probabilities can be derived from the PIR time cdf, already modeled in the previous sections. In fact, p_i, with $1 \leq i \leq \ell-1$, is the probability that the PIR is no larger than $i+1$ beaconing intervals, given that it is larger than i beaconing intervals (missing i beacons corresponds to a PIR time of $i+1$ beaconing interval). Thus we can write:

$$1 - p_i = \mathbb{P}[PIR > i+1 | PIR > i] \ , \tag{3}$$

which implies

$$p_i = 1 - \frac{\mathbb{P}[PIR > i+1]}{\mathbb{P}[PIR > i]} \tag{4}$$

The case $i = 0$ corresponds to the probability that two consecutive beacons are received, i.e.:

$$p_0 = 1 - \mathbb{P}[PIR > 1] \tag{5}$$

The corresponding transition matrix is:

$$\mathbf{M}=\begin{bmatrix} p_0 & 1-p_0 & 0 & 0 & \dots & 0 & 0 \\ p_1 & 0 & 1-p_1 & 0 & \dots & 0 & 0 \\ p_2 & 0 & 0 & 1-p_2 & \dots & 0 & 0 \\ \vdots & \vdots & \vdots & \vdots & \ddots & \vdots & \vdots \\ p_{\ell-1} & 0 & 0 & 0 & \dots & 1-p_{\ell-1} & 0 \\ 0 & 0 & 0 & 0 & \dots & 0 & 1 \end{bmatrix} \tag{6}$$

The expected absorbing time is computed through matrix $\mathbf{Q}$, which is obtained from matrix $\mathbf{M}$ by deleting the rows and columns corresponding to the absorbing states (in our case, therefore, by deleting the last row and the last column). The $\ell \times 1$ column vector $\mathbf{T}$ contains, as the i–th element, the expected absorbing time starting from state S_{i-1}. It is derived as $\mathbf{T} = (\mathbf{I}_\ell - Q)^{-1}\mathbf{1}_\ell$, where $\mathbf{I}_\ell$ is the identity matrix of size ℓ and $\mathbf{1}_\ell$ is a column vector of length ℓ with all elements equal to 1. Since we are interested in computing the average time T_{bo}^H between two subsequent black-out events, we have that $T_{bo}^H = (\mathbf{T}(1) - \ell)T_B$, where we need to subtract ℓ to identify the instant before the black-out beginning, while T_B is the beaconing interval. Given the particular structure of $\mathbf{M}$, a closed form expression also exists:

$$T_{bo}^H = \left(\sum_{i=0}^{\ell-1} \prod_{j=\ell-1-i}^{\ell-1} \frac{1}{1-p_j} - \ell \right) T_B \tag{7}$$

The inter-black out time estimate derived from this model can be considered an upper bound to the actual one. In fact, the channel time correlation is significant over several beaconing times. In our model, this means that the transition probabilities among the states closer to the absorbing state S_ℓ are more accurate. In fact, the probability of going from S_i to S_{i+1} implicitly takes into account the entire Markov process evolution in the previous i states. Conversely, this is not true for the states closer to S_0, and especially for S_0 itself. In fact, when the process enters S_0, it completely loses the memory about the previous state which, however, is likely to have a strong influence on the transition to the next state. Intuition suggests that if several beacons have been lost before the last reception, the probability of losing the next one is higher than in the case of having successfully received also the previous beacons. When computing the expected value, it results higher than in reality, since as S_0 is reached, the model forgets the consecutive losses of the previous beacons. As confirmed by the results reported in the following, T_{bo}^H is an upper bound of the measured inter-black out time, which becomes tighter when the channel conditions are bad (e.g., relatively high contention), and state S_0 is visited fewer times.

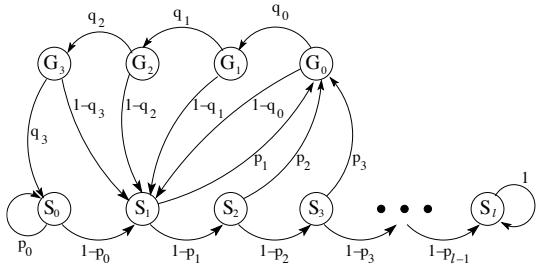

Fig. 10. Graphical representation of the MC modeling process $\mathcal{L}$, with $k = 3$.

A more refined MCM can be defined, by keeping memory of past states also when beacons are successfully received. A simple way to do this is to introduce some states G_i, with $0 \leq i \leq k$. The system is in state G_i when the previous i beacons have been correctly received. The number of additional states k can be tuned (it is set to 9 in the following), and we call $\mathcal{L}$ the new Markov process, which is reported in Figure 10. Whenever a beacon is lost, process $\mathcal{L}$ behaves as $\mathcal{H}$; however, upon reception of a beacon, it moves to state G_0, rather than S_0. The process then proceeds along the G_i states as long as beacons are received, finally arriving in S_0. If instead a beacon is lost, the process moves to S_1, as before. This second model, which better represents the channel behavior after a packet loss, requires in turn additional information. If we call N_b the number of correctly received consecutive beacons between two packet losses, the probabilites q_i's can be found based on the ccdf of the distribution of N_b:

$$q_0 = \mathbb{P}[N_b > 1], \qquad q_i = \frac{\mathbb{P}[N_b > i]}{\mathbb{P}[N_b > i-1]} \ .$$

The derivation of the corresponding transition matrix $\mathbf{M}_L$ is straightforward. By calling $\mathbf{Q}_L$ the matrix obtained by removing the row and the column corresponding to S_ℓ, the vector of the average absorbing times of the process is $\mathbf{T}_L = \left(\mathbf{I}_{\ell+k+1} - \mathbf{Q}_L\right)^{-1}\mathbf{1}_{\ell+k+1}$, and the expected time between two consecutive blackouts is $T_{bo}^L = (\mathbf{T}_L(1) - \ell)T_B$. We first notice that $T_{bo}^L < T_{bo}^H$. In fact, the two processes follow the same behavior along states S_i's. Nonetheless,

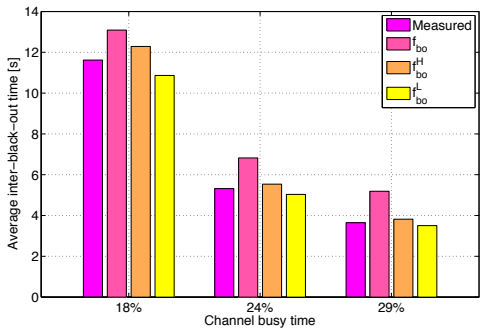

Fig. 11. Avg inter-black out time on the link (V_0, V_2), for different values of the congestion level R (expressed as a CBT value).

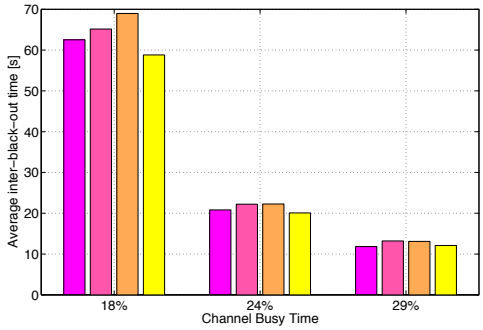

Fig. 12. Avg inter-black out time on the link $(V_0, V_2)_{MH}$, when multi-hop beaconing is enabled, for different values of the Congestion level R (expressed as a CBT value).

when a beacon is received, process $\mathcal{L}$ moves to state S_0, while process $\mathcal{H}$ moves to state G_0. Now, it can be shown that $q_0 < p_0$. In fact, both represent the probability of receiving the following beacon and are obtained from the measurements collected during the experiments; however, while p_0 is measured over all the received beacons, q_0 is measured only over the beacons received immediately after a packet loss. Since the channel is time correlated, it follows that the probability of receiving two consecutive beacons after a packet loss is lower than the unconditioned probability of receiving two consecutive beacons.

Also the values obtained through process $\mathcal{L}$ are approximated. In fact, memory is lost whenever the process enters state G_0 and state S_1. This is more evident for sparse beacon losses, since from S_1 the only available transition is to G_0. In this state, the packet loss probability is higher than in reality, since it is averaged over all the beacons received after a loss. It follows that f^L_{bo} is often even lower than the actual expected time interval between black-out events, as confirmed by the results.

We report in figures 11 and 12 the values of the inter-black out time computed with the three models, compared with the measured value. The plots refer to link (V_0, V_2) (single- and multi-hop) and different congestion levels. The results confirm that T_{bo}, assuming independence between black-out events, always gives an optimistic estimate of the true inter-black out time, independently of the congestion level. Conversely, both T^H_{bo} and T^L_{bo}, which take into account channel correlation, predict inter black-out times increasingly closer to the measured values as congestion level increases. This is due to the fact that correlation is better modeled during periods with no successful beacon reception, which happen more frequently when congestion is high.

As explained above, we always have $T^H_{bo} > T^L_{bo}$; while the former is also higher than the effective black-out frequency, the latter is instead always below. This last inequality is not necessarily true, but in most cases T^H_{bo} and T^L_{bo} can be effectively used to identify an upper and a lower bound to the actual inter-black out time, respectively.

We conclude with a comment on the notable effect of congestion on inter-black out time: when CBT is increased from about 18% to about 29%, the inter-black out time is reduced of a factor 4 in the (V_1, V_0) link, and of a factor 3 in the (V_0, V_2) link. Thus, an *increase of about* 10% *of the observed CBT causes a 3- to 4-fold increase of black-out frequency*. This finding experimentally confirms the necessity of keeping the congestion level under strict control, in accordance with recommendations from standardization bodies: for instance, ETSI recommends a CBT $\leq 25\%$ [4]. Interestingly, *multi-hop beaconing can be exploited to substantially reduce occurrence of black-out events, also in presence of congestion*: comparing the values reported in figures 11 and 12, we observe that the inter-black out time at CBT 29% is increased of a factor 2.5 when multi-hop beaconing is used on link (V_0, V_2), with a corresponding decrease of black-out frequency.

VIII. Application to Forward Collision Warning

In this section, we show how the measurement-based models presented in this paper can be used to estimate the reliability of a forward collision warning application in presence of different congestion levels, and to assess the positive impact of congestion control techniques on application reliability.

A forward collision warning application warns the driver when a rear-end collision danger is detected, so to reduce the risk of an accident. In this application, a vehicle needs to constantly monitor the status of forward vehicles. Considering two vehicles A (back) and B (front), a rear-end collision would be avoided if the PIR time measured at A referring to the beacons sent by B is kept below a certain threshold. Upper bounding the PIR time ensures that A constantly keeps a relatively "fresh" information about the status of vehicle B, allowing for a prompt detection of potentially dangerous conditions onboard vehicle A. The *reliability* of the forward collision warning application is defined in [14] as the percentage of time during which the application requirement is satisfied.

The exact value of the PIR time requirement onboard vehicle A depends on parameters such as inter-vehicle distance, speed, vehicle length, etc. – see [14]. According

to the data reported in [14], the upper bound on the PIR time typically varies between 0.5 and 2.7 sec. Without loss of generality, in the following we assume a required upper bound on the PIR time of 1 sec, corresponding, e.g., to the upper bound requested when the two vehicles drive at 80 km/h at a distance of 60 m.

Let us now apply the measurement-based models presented in this paper to estimate the reliability of a forward collision warning application running on vehicle V_2, considering the link (V_0, V_2). Setting the upper bound on the PIR time to 1 sec, we have that the application requirements are not satisfied whenever a black-out (BO) event occurs. Hence, the application reliability can be estimated by estimating the frequency and average duration of a BO event.

Link	**CBT=**18%	**CBT=**24%	**CBT=**29%
(V_0, V_2)	1.28 sec	1.42 sec	1.44 sec
$(V_0, V_2)_{MH}$	1.18 sec	1.23 sec	1.22 sec

TABLE I
AVERAGE BO DURATION IN THE (V_0, V_2) LINK.

The MCM model predicts that the BO frequency with medium congested channel (CBT=24%) is about 1 event every 5.2 sec (*cfr* Figure 11). Considering that the average duration of a BO event with that level of congestion is 1.42 sec – see Table I, we have that the application reliability with $CBT = 24\%$ is about 63%.[4] If multi-hop forwarding of beaconing information is used, the BO frequency is reduced to about 1 event every 20 sec (*cfr* Figure 12), and the BO duration is 1.23 sec, which increases application reliability to 94%. Thus, *multi-hop forwarding of beaconing information can be used to substantially increase application reliability in presence of moderate channel congestion*.

Our derived models can be used also to estimate the benefits of congestion control on application reliability. More specifically, we consider a scenario in which the forwarding collision warning application co-exists with a "congestion controlled" lane change assistance application as the one introduced in [15]. The application introduced in [15] adapts its transmission parameters based on contextual information obtained from surrounding vehicles to reduce congestion on the wireless channel. The authors of [15] report that the CBT can be reduced[5] from about 25% to about 15% when contextual information is used to control congestion. Thanks to congestion control performed by the lane changing application, the reliability of the forward collision warning application is increased from about 63% without congestion control to about 89% with congestion control. If multi-hop forwarding of beaconing information is used by the forward collision warning application, application reliability is increased from about 94% without congestion control to about 98% with congestion control.

[4]Although the reliability values cannot be directly compared due to different experimental setups, it is interesting to observe that the estimated reliability in presence of congestion is much lower than the values above 80% reported in [14] *in absence of channel congestion*.

[5]The data refers to a configuration with 3 lanes per direction, and a density of 9.6 veh/km/lane.

IX. CONCLUSIONS

In this paper, we have presented the first measurement-based study of the PIR time in presence of channel congestion. Our study has revealed the profound impact of congestion on the PIR time, and on the resulting application-level reliability. Another major finding of this study is showing the effectiveness of multi-hop beaconing in lessening the negative impact of congested channel conditions on beaconing performance and, in turn, on application-level reliability.

Possible future research directions include performing measurement-based studies with larger deployments, in order to understand whether and, possibly, to what extent, the complex dynamic of a large scale CSMA/CA network impacts the results presented in this paper.

REFERENCES

[1] F. Bai, D.D. Stancil, H. Krishnan, "Toward Understanding Characteristics of Dedicated Short Range Communications (DSRC) From a Perspective of Vehicular Network Engineers", *Proc. ACM Mobicom*, pp. 329–340, 2010.

[2] "Standard Specification for Telecommunications and Information Exchange Between Roadside and Vehicle Systems - 5Ghz Band Dedicated Short Range Communications (DSRC)", *ASTM E2212-03*, 2003.

[3] T. ElBatt, S.K. Goel, G. Holland, H. Krishnan, J. Parikh, "Cooperative Collision Warning Using Dedicated Short Range Wireless Communications", *Proc. ACM VANET*, 2006.

[4] ETSI, "Decentralized Congestion Control Mechanisms for ITS Operating in the 5GHz Range", ETSI TS 102 687, 2011.

[5] J. Gozalves, M. Sepulcre, R. Bauza, "IEEE 802.11p Vehicle to Infrastructure Communications in Urban Environments", *IEEE Commun. Mag.*, Vol. 50, n. 5, pp. 176–183, 2012.

[6] K. Hong, D. Xing, V. Rai, J. Kenney, "Characterization of DSRC Performance as a Function of Transmit Power", *Proc. ACM VANET*, pp. 63–68, 2009.

[7] C.-L. Huang, Y.P. Fallah, R. Sengupta, H. Kirshnan, "Adaptive Intervehicle Communication Control for Cooperative Safety Systems", *IEEE Network*, Vol. 24, n. 1, pp. 6–13, 2010.

[8] D. Jiang, Q. Chen, L. Delgrossi, "Optimal Data Rate Selection for Vehicle Safety Communications", *Proc. ACM VANET*, pp. 30–38, 2008.

[9] J.B. Kenney, G. Bansal, C.E. Rohrs,"LIMERIC: a Linear Message Rate Control Algorithm for Vehicular DSRC Systems", *Proc. ACM VANET*, pp. 21–30, 2011.

[10] F. Librino, M.E. Renda, P. Santi, "Evaluating Multi-Hop Beaconing Forwarding Strategies for IEEE 802.11p Vehicular Networks, *Proc. IEEE Vehicular Networking Conf.*, 2013.

[11] T. Mangel, M. Michl, O. Klemp, H. Hartenstein, "Real-World Measurements of Non-Line-Of-Sight Reception Quality for 5.9Ghz IEEE 802.11p at Intersections", *Proc. Nets4Cars*, pp. 189–202, 2011.

[12] F. Martelli, M.E. Renda, G. Resta, P. Santi, "A Measurement-based Study of Beaconing Performance in IEEE 802.11p Vehicular Networks", *Proc. IEEE Infocom*, 2012.

[13] M. Sepulcre, J. Mittag, P. Santi, H. Hartenstein, J. Gozalvez, "Congestion and Awareness Control in Cooperative Vehicular Systems", *Proc. IEEE*, Vol. 99, pp. 1260-1279.

[14] M. Sepulcre, J. Gozalvez, "Experimental Evaluation of Cooperative Active Safety Applications based on V2V Communitcations", *Proc. ACM VANET*, pp. 13–20, 2012.

[15] M. Sepulcre, J. Gozalvez, J. Harri, H. Hartenstein, "Contextual Communications Congestion Control for Cooperative Vehicular Networks", *IEEE Trans. on Wireless Communications*, Vol. 10, n. 2, pp. 385–389, 2011.

[16] M. Torrent-Moreno, D. Jiang, H. Hartenstein, "Broadcast Reception Rates and Effects of Priority Access in 802.11-based Vehicular Ad Hoc Networks", *Proc. ACM VANET*, pp. 11–18, 2004.

[17] M. Torrent-Moreno, J. Mittag, P. Santi, H. Hartenstein, "Vehicle-to-Vehicle Communication: Fair Transmit Power Control for Safety-Critical Information", *IEEE Trans. on Vehicular Technology*, Vol. 58, n. 7, pp. 3684–3703, 2009.